Date of publication xxxx 00, 0000, date of current version xxxx 00, 0000.

Digital Object Identifier 10.1109/ACCESS.2017.DOI

Modified SNR Gap Approximation for Resource Allocation in LDPC-coded Multicarrier Systems

ADRIAAN SULS[1], (Student, IEEE), JEROEN VERDYCK[2], (Student, IEEE), MARC MOONEN[2], (Fellow, IEEE), and MARC MOENECLAEY[1], (Fellow, IEEE)

[1]Dept. of Telecommunications and Information Processing, Ghent University, Belgium

[2]STADIUS Center for Dynamical Systems, Signal Processing and Data Analytics, KU Leuven, Belgium

Corresponding author: Adriaan Suls (e-mail: adriaan.suls@ugent.be)

This research work was carried out in the frame of Fonds de la Recherche Scientifique - FNRS and Fonds Wetenschappelijk Onderzoek - Vlaanderen FWO EOS Project no 30452698 ’(MUSE-WINET) MUlti-SErvice WIreless NETwork’ (Ghent University, KU Leuven), Research Project FWO no G.0B1818N ’Real-time adaptive cross-layer dynamic spectrum management for fifth generation broadband copper access networks’ (KU Leuven), VLAIO O&O Project nr. HBC.2016.0055 ’5GBB Fifth generation broadband access’ (Ghent University, KU Leuven), Research Project FWO nr. G.013917N ’Advanced MIMO channel modeling and signal processing for high-bitrate chip-to-chip interconnects prone to manufacturing variability’ (Ghent University). The scientific responsibility is assumed by its authors.

ABSTRACT The signal-to-noise ratio (SNR) gap approximation provides a closed-form expression for the SNR required for a coded modulation system to achieve a given target error performance for a given constellation size. This approximation has been widely used for resource allocation in the context of trellis-coded multicarrier systems (e.g., for digital subscriber line communication). In this contribution, we show that the SNR gap approximation does not accurately model the relation between constellation size and required SNR in low-density parity-check (LDPC) coded multicarrier systems. We solve this problem by using a simple modification of the SNR gap approximation instead, which fully retains the analytical convenience of the former approximation. The performance advantage resulting from the proposed modification is illustrated for single-user digital subscriber line transmission.

INDEX TERMS LDPC codes, Resource Allocation, Channel Coding, Information Theory, Wireless Networks, OFDM

I. INTRODUCTION

Resource allocation (RA) improves the performance of multicarrier systems by adapting the transmission parameters to the actual channel conditions. In this contribution we consider multicarrier modulation which maintains subcarrier orthogonality on dispersive channels; this orthogonality can be achieved by means of a cyclic prefix, in which case the resulting modulation is referred to as orthogonal frequency-division multiplexing (OFDM) and discrete multi-tone (DMT) in wireless and wireline applications, respectively.

In these multicarrier systems, an RA algorithm determines the number of coded bits per symbol μ_n and the transmit energy E_n for each subcarrier $n \in \{1, \dots, N\}$. The considered RA algorithm aims at solving the rate-adaptive RA problem, consisting of maximizing the data rate subject to both a maximum aggregate transmit power (ATP) constraint and a maximum bit error rate (BER) constraint. As μ_n can only take on integer values, the rate-adaptive RA problem is a mixed integer program. Furthermore, the BER constraint will be enforced by imposing a lower bound $\gamma_{\mathrm{thr}}(\mu)$ on the signal-to-noise ratio (SNR), that depends on the constellation size (expressed in bits) μ, allowing the BER constraint to be replaced by a simple per-subcarrier minimum SNR constraint $\gamma_n \geq \gamma_{\mathrm{thr}}(\mu_n)$.

Many algorithms have been proposed that optimally solve this rate-adaptive RA problem. Early RA algorithms focused on single-user multicarrier systems and relied on greedy bit adding (subtracting) [1, 2]. These bit adding (subtracting) algorithms were shown to be optimal in [3, 4]. A computationally more efficient RA algorithm was proposed in [5], which relied on solving the Lagrange dual of the rate-adaptive RA problem.

When extended to more involved multi-user systems, such Lagrange dual-based RA algorithms are still able to find the optimal solution to the rate-adaptive RA problem [6, 7, 8]. However, the computational complexity of these Lagrange dual-based algorithms scales badly with an increasing number of users. On the other hand, the computational complexity of the multi-user extension of the greedy bit adding (subtracting) algorithms does scale well with an increasing number of users [9, 10]. This low computational cost however comes at the expense of optimality, as greedy multi-user RA algorithms cannot guarantee a globally optimal solution.

Another set of methods to solve the RA problem are based on the SNR gap approximation (SGA), originally introduced in [11]. These algorithms consider the bit loading μ_n to be a continuous variable, and employ a smooth approximation of the SNR threshold constraint $\gamma_n \geq \gamma_{\text{stgap}}(\mu_n)$, where $\gamma_{\text{stgap}}(\mu_n)$ is the standard SGA of $\gamma_{\text{thr}}(\mu_n)$. An early single-user RA algorithm employing the SGA can be found in [12]. The SGA simplifies the mathematical structure of the RA problem, thereby enabling the design of low-complexity multi-user RA algorithms achieving close-to-optimal performance [13, 14, 15, 16, 17, 18].

As SGA-based algorithms yield non-integer values for μ_n, they require a discretization method to map the obtained continuous RA to a discrete RA. One such discretization method consists of rounding μ_n with a custom threshold α and recalculating E_n such that the minimum SNR constraints $\gamma_n \geq \gamma_{\text{stgap}}(\mu_n)$ are strictly satisfied [3], where α is chosen such that the ATP constraints are tight. Another common discretization method consists of rounding μ_n to the nearest integer, recalculating E_n, and employing bit adding (subtracting) to tighten the ATP constraints [19, 20, 21]. When applied to single-user systems, this discretization method finds the optimal solution to the discrete rate-adaptive RA problem with SGA-based SNR threshold constraints $\gamma_n \geq \gamma_{\text{stgap}}(\mu_n)$ [22].

While the standard SGA $\gamma_{\text{stgap}}(\mu_n)$ from literature is sufficiently accurate for multicarrier systems with uncoded transmission or trellis-coded modulation (TCM), we show in this contribution that its use in RA for low-density parity-check (LDPC) codes gives rise to a considerable violation of the BER constraint at large SNR, and to a rate loss at small SNR. To avoid these shortcomings, we present a modified SGA which is suitable for LDPC-coded modulation, and retains the analytical flexibility of the conventional approximation.

This contribution is organized as follows. In section II the multicarrier system and the main transmission parameters are presented. In section III, several SGAs are introduced, and their accuracy is assessed for LDPC-coded modulation. The RA algorithms based on the SNR thresholds and on the SGAs are outlined in section IV. The numerical results in section V show the effect of the various RA algorithms on the resulting information bitrate and BER performance of a single-user digital subscriber line (DSL) communication system. Finally, conclusions are drawn in section VI.

Throughout this contribution, X_{dB} represents the value in dB of a power ratio X, i.e. , $X_{\text{dB}} = 10\log_{10}(X)$; $\mathbf{1}_N$ denotes the all-ones vector with N components.

II. SYSTEM DESCRIPTION

We consider the single-user transmission of coded QAM data symbols over a time-invariant channel using multicarrier modulation with N subcarriers. The QAM symbols result from applying a sequence of information bits to a binary encoder, and mapping the coded bits to the proper constellation points. In the k-th multicarrier symbol $\mathbf{x}(k) = (x_1(k), ..., x_N(k))$, the n-th subcarrier ($n \in \{1, ..., N\}$) conveys a symbol $x_n(k)$ from a normalized (i.e. $\mathbb{E}\left[|x_n(k)|^2\right] = 1$) M_n-QAM constellation, representing $\mu_n = \log_2(M_n)$ coded bits, with $\mu_n \in \{1, 2, ..., \mu_{\max}\}$.[†] We refer to $\boldsymbol{\mu} = (\mu_1, ..., \mu_N)$ as the bitloading vector.

The corresponding received signal is given by

$$y_n(k) = h_n x_n(k) + w_n(k) \tag{1}$$

where $w_n(k)$ is complex-valued zero-mean Gaussian noise with $\mathbb{E}\left[|w_n(k)|^2\right] = N_{0,n}$, and h_n represents the channel gain on the n-th subcarrier. We express the SNR (linear scale) γ_n as $\gamma_n = \beta_n E_n$, where $\beta_n = |h_n|^2/N_{0,n}$ and E_n are the power gain-to-noise ratio and transmitted symbol energy on the n-th subcarrier. The vector $\mathbf{E} = (E_1, ..., E_N)$ represents the transmitted symbol energies and the vector $\boldsymbol{\gamma} = (\gamma_1, ..., \gamma_N)$ denotes the SNR profile. To limit latency, practical multicarrier systems apply coding across subcarriers; hence, in general the QAM symbols that correspond to a codeword have different constellation sizes and different SNRs, as they are sent over different subcarriers.

Although the prime focus is on LDPC codes, we will also briefly revisit TCM and uncoded modulation, as the SGA is widely used in RA algorithms for systems employing these modulations.

III. SNR GAP APPROXIMATIONS

For multicarrier modulation with uniform bitloading and uniform SNR profile ($\boldsymbol{\mu} = \mu\mathbf{1}_N$ and $\boldsymbol{\gamma} = \gamma\mathbf{1}_N$), we define the SNR thresholds $\{\gamma_{\text{thr}}(\mu), \mu = 1, ..., \mu_{\max}\}$ for a given code such that the BER equals some target value BER_{ref} when $\gamma = \gamma_{\text{thr}}(\mu)$. These thresholds will be used in section IV-A to perform RA for given power gain-to-noise ratios $(\beta_1, ..., \beta_N)$, yielding non-uniform bitloading and non-uniform SNR profile in general.

The SNR gap (in dB) to capacity for a given code and given values of γ and μ is defined as

$$\Gamma_{\text{gap,dB}}(\mu) = \gamma_{\text{dB}} - 10\log_{10}(2^{\mu_{\text{info}}} - 1) \tag{2}$$

where μ_{info} denotes the number of information bits transmitted per channel use, the value of which depends on μ and on the considered code. The factor $(2^{\mu_{\text{info}}} - 1)$ in (2) equals the SNR needed to support the transmission without

[†]We restrict our attention to the M-QAM constellations from the G.fast standard [23], which are 2-QAM (equivalent to BPSK), 8-QAM (containing the 8 even-numbered constellation points from 16-QAM), square-QAM ($M = 2^2, 2^4, 2^6, ...$) and cross-QAM ($M = 2^5, 2^7, 2^9, ...$).

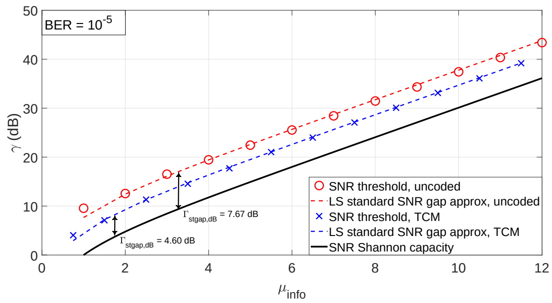

Figure 1: The LS standard SGA provides a good fit with the SNR thresholds for uncoded transmission and for TCM.

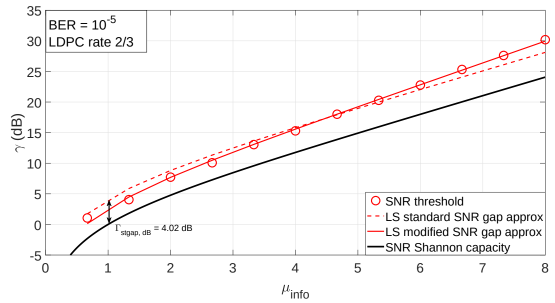

Figure 2: For LDPC coding, the LS modified SGA outperforms the LS standard SGA in terms of fitting the SNR thresholds.

errors at a rate of μ_{info} bits per channel use, according to the Shannon capacity formula. This definition of $\Gamma_{\text{gap,dB}}$ corresponds to the "normalized SNR" introduced in [11]. For given μ, the SNR gap at BER = BER_{ref} is obtained by substituting in (2) γ_{dB} by $\gamma_{\text{thr,dB}}(\mu)$; this gap depends on μ. The standard SGA [24] is an approximation of the SNR thresholds $\gamma_{\text{thr}}(\mu)$ for various μ using (2), under the assumption that $\Gamma_{\text{gap,dB}}(\mu)$ is not a function of μ, i.e, $\Gamma_{\text{gap,dB}}(\mu) = \Gamma_{\text{stgap,dB}}$ irrespective of μ. The resulting standard SGA is denoted $\gamma_{\text{stgap,dB}}(\mu)$, and is given by

$$\gamma_{\text{stgap,dB}}(\mu) = \Gamma_{\text{stgap,dB}} + 10\log_{10}\left(2^{\mu_{\text{info}}} - 1\right) \quad (3)$$

When $2^{\mu_{\text{info}}} \gg 1$, (3) can be approximated as $\gamma_{\text{stgap,dB}}(\mu) \approx \Gamma_{\text{stgap,dB}} + 3\mu_{\text{info}}$, indicating a linear increase of 3 dB per information bit. In the following, we investigate the accuracy of this approximation for uncoded transmission, TCM and LDPC-coded modulation.

We determined by means of Monte Carlo (MC) simulations the SNR thresholds $\gamma_{\text{thr,dB}}$ (in dB) at $\text{BER}_{\text{ref}} = 10^{-5}$ for uncoded transmission, the 16-state 4-dimensional trellis code from [23, p. 106], and the rate-2/3 (1440, 960) LDPC code from the G.hn standard [25], for $\mu = 1, ..., 12$. The relation between μ and μ_{info} is $\mu_{\text{info}} = \mu$ for uncoded transmission, $\mu_{\text{info}} = \mu - \frac{1}{2}$ for the trellis code, and $\mu_{\text{info}} = \frac{2}{3}\mu$ for the LDPC code. We show in Fig. 1 (for uncoded transmission and TCM) and Fig. 2 (for LDPC-coded modulation) the SNR thresholds along with the SNR according to the Shannon capacity formula, all as a function of μ_{info}. Also displayed is the least-squares (LS) standard SGA (3), where $\Gamma_{\text{stgap,dB}}$ is selected such that $\gamma_{\text{stgap,dB}}$ is a least-squares (LS) approximation of $\gamma_{\text{thr,dB}}$ for $\mu = 1, ..., 12$; this yields $\Gamma_{\text{stgap,dB}} \approx$7.67 dB, 4.60 dB and 4.02 dB, for uncoded transmission and for the considered TCM and LDPC-coded modulation, respectively.

It follows from Fig. 1 that, for uncoded transmission and TCM, the threshold values $\gamma_{\text{thr,dB}}$ exhibit an SNR gap to capacity which is nearly independent of μ_{info}. The threshold values are well approximated by the LS standard SGA (3), especially for $\mu \geq 2$, where the approximation error magnitudes for uncoded transmission and TCM are less than 0.5 dB and 0.25 dB, respectively. The good agreement between the threshold values and the standard SNR gap approximation for uncoded transmission and TCM can be shown to result from their error performance being mainly determined by the minimum Euclidean distance between symbol sequences [24, 26].

It is seen from Fig. 2 that the situation is drastically different for LDPC coding. We observe that the SNR gap to capacity cannot be considered constant, but instead gets larger with increasing μ_{info}; this behavior can be attributed to the fact that the error performance of LDPC codes is mainly governed by the mutual information between a coded bit and its corresponding log-likelihood ratio [27, 26], rather than the minimum Euclidean distance between symbol sequences. The LS standard SGA (3) fails to accurately describe the relation between $\gamma_{\text{thr,dB}}$ and μ_{info}, basically because (3) underestimates the actual slope of $\gamma_{\text{thr,dB}}$ versus μ_{info}. The LS standard SGA yields too small constellations at low SNR (giving rise to reduced information bitrate) and too large constellations at high SNR (giving rise to increased BER).

For LDPC-coded modulation we propose to include in (3) a slope correction factor a, such that a better fit to the SNR thresholds results; more specifically, we introduce

$$\gamma_{\text{modgap,dB}} = \Gamma_{\text{modgap,dB}} + 10\log_{10}(2^{\mu_{\text{info}}a} - 1) \quad (4)$$

which we refer to as the modified SGA; for $a = 1$, (4) reduces to the standard SGA (3). For $2^{\mu_{\text{info}}a} \gg 1$, (4) is approximated as $\gamma_{\text{modgap,dB}}(\mu) \approx \Gamma_{\text{stgap,dB}} + 3a\mu_{\text{info}}$ indicating a linear increase of $3a$ dB per information bit. The slope correction factor a can be selected to obtain a better match to $\gamma_{\text{thr,dB}}$ for the considered LDPC code. With $(\Gamma_{\text{modgap,dB}}, a) \approx$ (1.5 dB, 1.18) providing the LS fit of the modified SGA to the SNR thresholds for the considered LDPC code, we observe from Fig. 2 that the resulting LS modified SGA (4) is much more accurate than the LS standard SGA (3).

For some constellation sizes, the LS standard SGA and LS modified SGA yields SNR values that are smaller than the actual SNR threshold. Hence, when the bitloading is

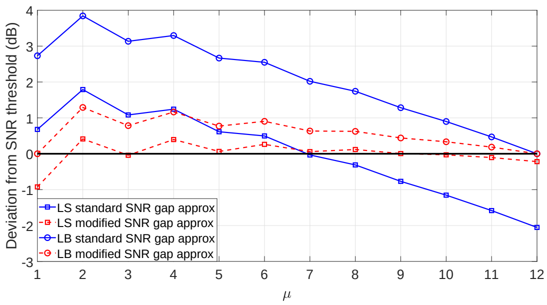

Figure 3: Deviation of SGAs from SNR thesholds for rate-2/3 LDPC coding

μ	Number of coded bits in QAM symbol
μ_{info}	Number of information bits in QAM symbol
$\gamma_{\text{thr}}(\mu)$	SNR threshold corresponding to BER $=$ BER_{ref}
$\gamma_{\text{stgap}}(\mu)$	SNR threshold corresponding to standard SGA (3) (*)
$\gamma_{\text{modgap}}(\mu)$	SNR threshold corresponding to modified SGA (4) (*)
$\Gamma_{\text{stgap,dB}}$	Parameter determining the standard SGA (*)
$(\Gamma_{\text{modgap,dB}}, a)$	Parameters determining the modified SGA (*)
	(*) a subscript "LS" or "LB" can be added to indicate how the SGA has been fitted to $\gamma_{\text{thr}}(\mu), \mu = 1, ..., \mu_{\max}$

Table 1: SGA symbols summary

based on these LS SGAs, an increased BER for these constellations results. This BER increase can be avoided by selecting the values of $\Gamma_{\text{stgap,dB}}$ and $(\Gamma_{\text{modgap,dB}}, a)$ such that (3) and (4) are LS approximations under the restriction that for each value of μ the SNR threshold is a lower bound (LB) on the corresponding approximation. This results in what we call the LB standard SGA and LB modified SGA; the LB standard SGA has been used in [27]. For the considered LDPC code, the LB SGAs are characterized by $\Gamma_{\text{stgap,dB}} \approx$ 6.1 dB in (3) and $(\Gamma_{\text{modgap,dB}}, a) \approx$ (2.6 dB, 1.14) in (4), respectively. However, compared to the case where the bitloading is based on the true SNR thresholds, this approach gives rise to smaller constellation sizes (and, hence, to a reduced information bitrate). Fig. 3 shows the deviation of the considered approximations from the SNR threshold, as a function of the bitloading μ. We observe that the LB SGAs by construction give rise to a non-negative deviation, and that the deviations are much larger for the standard than for the modified SGAs. The main symbols related to the various SGAs are listed in Table 1.

Table 2 shows the parameters $\Gamma_{\text{stgap,dB}}$ and $(\Gamma_{\text{modgap,dB}}, a)$ for different LDPC codes from the G.hn standard, where we introduced the subscripts LS and LB to refer to the corresponding type of SGA. We observe that a_{LS} increases with decreasing code rate, which indicates that the mismatch, between the actual SNR thresholds and those resulting from the standard SGAs, gets larger for smaller code rates. Consequently, when the standard SGA is used, smaller code rates require a larger difference $\Gamma_{\text{LB,stgap,dB}} - \Gamma_{\text{LS,stgap,dB}}$

(N_c, K_c)	**(1152, 960)**	**(1440, 960)**	**(1920, 960)**
Code rate	5/6	2/3	1/2
$\Gamma_{\text{LS,stgap,dB}}$	3.76	4.02	4.23
$\Gamma_{\text{LB,stgap,dB}}$	4.70	6.02	6.79
$\Gamma_{\text{LS,modgap,dB}}$	2.95	1.55	0.42
a_{LS}	1.05	1.18	1.35
$\Gamma_{\text{LB,modgap,dB}}$	4.24	2.64	1.34
a_{LB}	1.02	1.14	1.32

Table 2: SGA parameters for (N_c, K_c) LDPC code

to avoid that the BER exceeds BER_{ref}.

IV. RESOURCE ALLOCATION FOR LDPC CODING

We now consider the RA problem for LDPC-coded multicarrier transmission operating on a channel with arbitrary power gain-to-noise ratios $(\beta_1, ..., \beta_N)$. We aim to maximize the information bitrate associated with the multicarrier system, under maximum BER and maximum transmit energy constraints. As for a (N_c, K_c) LDPC code the ratio of information bits to coded bits is given by $r_c = K_c/N_c$, the RA problem is formulated as:

$$\underset{\boldsymbol{\mu}, \mathbf{0} \preceq \mathbf{E}}{\text{maximize}} \quad N_{\text{info}} \tag{5a}$$

$$\text{subject to} \quad \mu_n \leq f_b(\beta_n E_n), \forall n \in \{1, \dots, N\} \tag{5b}$$

$$\sum_{n=1}^{N} E_n \leq E_{\text{tot}}^{\max} \tag{5c}$$

where $N_{\text{info}} = r_c \sum_{n=1}^{N} \mu_n$ is the number of information bits in the multicarrier symbol, and $\mathbf{0} \preceq \mathbf{E}$ indicates that all components of $\mathbf{E}$ must be nonnegative. In (5c), $\sum_{n=1}^{N} E_n$ and $E_{\text{tot}}^{\max}$ denote the aggregate transmit energy per multicarrier symbol, and its maximum allowed value, respectively; in (5b), f_b is the bitloading function defining the maximum number of coded bits as a function of the SNR. This bitloading function f_b is then chosen such that $\text{BER} \leqslant \text{BER}_{\text{ref}}$, and can be obtained either from the exact SNR thresholds $\gamma_{\text{thr}}(\mu)$ or from the modified SGA (4), with μ_{info} replaced by $r_c\mu$. The choice of bitloading function directly determines which algorithms are available to solve problem (5).

A. THRESHOLD-BASED RA

When considering the exact SNR thresholds, f_b in (5b) is the maximum value of μ satisfying $\gamma_{\text{thr}}(\mu) \leq \gamma$. The resulting optimization problem is a mixed integer program, which can be solved by means of a greedy algorithm [1, 3]; however, convergence will typically be rather slow. Considerably faster algorithms are available which are based on Lagrange dual decomposition; the solution method is detailed in [5].

A major advantage of threshold-based RA is that one can expect the resulting BER to be very close to the target value BER_{ref}, as will be confirmed in Section V. Moreover, threshold-based RA methods are available for many other settings, e.g., multi-user settings for the interference channel [6], the multiple access channel [7] and the broadcast channel [8]. However, these methods tend to scale badly in multi-user settings, as their numerical complexity grows exponentially with the number of users.

B. MODIFIED SGA-BASED RA

When performing RA based on the SGA, the components of the bitloading vector $\boldsymbol{\mu}$ are considered continuous (rather than discrete) variables, which allows using efficient analytical optimization methods. The bitloading function corresponding to the modified SGA (4) is

$$f_{\mathrm{b}}(\gamma) = (r_{\mathrm{c}} a)^{-1} \log_2 \left(1 + \Gamma_{\mathrm{modgap}}^{-1} \gamma\right) \tag{6}$$

Replacing in (6) the parameters $(a, \Gamma_{\mathrm{modgap}})$ by $(1, \Gamma_{\mathrm{stgap}})$, we obtain the bitloading function associated with the standard SGA as a special case. As a appears merely as a proportionality factor in (6), the solution method and the computational complexity for the modified SGA are the same as for the standard SGA, which is well documented in literature.

First, problem (5) with $f_{\mathrm{b}}(\gamma)$ given by (6) is solved using the well-known water-filling algorithm [24], yielding the optimum continuous bit allocation. Next, the globally optimal solution to the modified SGA-based discrete bitloading problem can be obtained by rounding the water-filling solution to the nearest integer and applying greedy bit adding/subtracting until the power constraints are tight [22].

Compared to the threshold-based methods from Section IV-A, it is to be expected that the obtained RA will result in a BER that is further away from the target value $\mathrm{BER}_{\mathrm{ref}}$, because $\gamma_{\mathrm{modgap}}(\mu) \neq \gamma_{\mathrm{thr}}(\mu)$. Moreover, when using the continuous approximation as in (6) as the basis for RA algorithms in a multi-user setting, global optimality cannot always be guaranteed. However, the strength of these SGA-based RA algorithms lies in the fact that they achieve close-to-optimal results while exhibiting exceedingly low complexity and being highly parallelizable [13, 15, 28]. Multi-user RA algorithms based on the standard SGA typically maximize the weighted sum of the per user information bitrates, and can be applied without modification to RA problems using the modified SGA as in (4). Finally, it is noted that the employed discretization method for obtaining an integer-valued bitloading can be readily generalized to multi-user settings [19].

V. NUMERICAL RESULTS

For the three LDPC codes from section III, we compare the RA performances (information bitrate and BER) resulting from using the SNR thresholds at $\mathrm{BER}_{\mathrm{ref}} = 10^{-5}$ and the four SGAs introduced above.

We consider single-user LDPC-coded multicarrier transmission over a twisted-pair (TP) access cable. The multicarrier system is according to the G.fast standard [23]: the multicarrier symbol rate R_{sy} and the subcarrier spacing F_{sub} equal 48 kHz and 51.75 kHz, respectively, and the

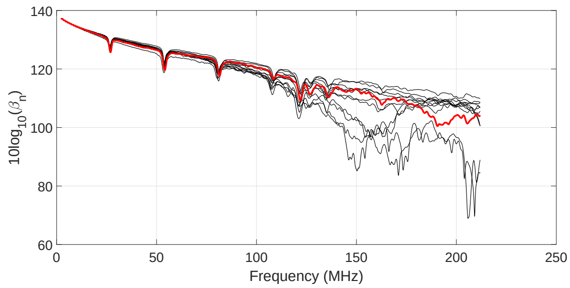

Figure 4: Power gain-to-noise ratios for the twelve TPs from [29]. Thick red line represents the 1st TP.

available subcarriers span the frequency interval (2.2 MHz, 212 MHz). We assume no crosstalk is present, and take only additive white Gaussian noise (with one-sided power spectral density of -140 dBm/Hz) into account. Transfer function measurements for twelve 104 m long TPs from the Dutch telecom operator KPN are available from [29]; Fig. 4 shows the corresponding power gain-to-noise ratios. The RA algorithms from section IV are executed under the constraint (5c) (which is equivalent to the ATP not exceeding a maximum value denoted $P_{\mathrm{tot}}^{\mathrm{max}} = E_{\mathrm{tot}}^{\mathrm{max}} F_{\mathrm{sub}}$) and the constraint $\mu_n \leq 12$ for $n = 1, ..., N$ on the constelllation sizes. This rather simple scenario is effective in illustrating the differences in BER performance and information bitrate among the various RA algorithms. Similar trends are expected to occur in more involved multi-user scenarios.

A. INFORMATION BITRATE OF SGA-BASED AND THRESHOLD-BASED RA

Fig. 5 shows the average (over all 12 TPs) information bitrate versus the maximum allowed ATP $P_{\mathrm{tot}}^{\mathrm{max}}$ for the threshold-based RA, using the LDPC code of rates 1/2, 2/3 or 5/6. The following observations can be made.

- In the limit for infinitely large $P_{\mathrm{tot}}^{\mathrm{max}}$, the average information bitrate becomes independent of $P_{\mathrm{tot}}^{\mathrm{max}}$. All subcarriers on all TPs are loaded with the μ_{max}-bit constellation, and the energy $E_n^{(l)}$ on the nth subcarrier from the lth TP is selected such that $\beta_n^{(l)} E_n^{(l)} = \gamma_{\mathrm{thr}}(\mu_{\mathrm{max}})$, where $\beta_n^{(l)}$ is the corresponding power gain-to-noise ratio. The resulting ATP $P_{\mathrm{tot}}^{(l)}$ on the lth TP is given by

$$P_{\mathrm{tot}}^{(l)} = \gamma_{\mathrm{thr}}(\mu_{\mathrm{max}}) F_{\mathrm{sub}} \sum_{n=1}^{N} \frac{1}{\beta_n^{(l)}} \tag{7}$$

  The corresponding number of information bits per subcarrier equals $\mu_{\mathrm{max}} r_{\mathrm{c}}$; hence, the information bitrate increases with the code rate. This asymtotic behavior occurs for $P_{\mathrm{tot}}^{\mathrm{max}} \geq \max_l P_{\mathrm{tot}}^{(l)}$, with $P_{\mathrm{tot}}^{(l)}$ given by (7). As $\gamma_{\mathrm{thr}}(\mu_{\mathrm{max}})$ is increasing with r_{c}, the asymptotic behavior starts at larger $P_{\mathrm{tot}}^{\mathrm{max}}$ when higher-rate codes are used.

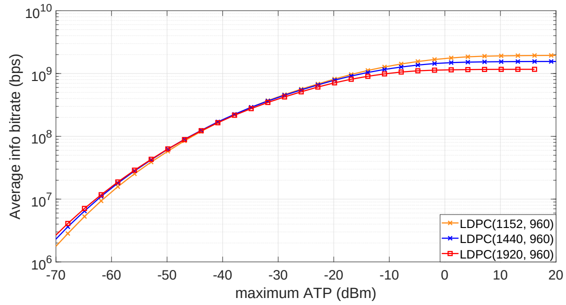

Figure 5: Average information bitrate for RA based on SNR thresholds.

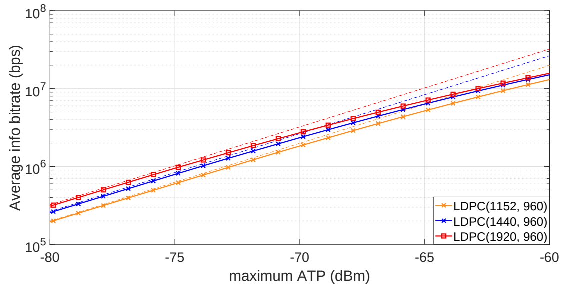

Figure 6: Average information bitrate at very small $P_{\rm tot}^{\rm max}$, for RA based on SNR thresholds. The dashed lines, corresponding to the approximation (8), are close to the true curves.

- In the limit for small $P_{\rm tot}^{\rm max}$, the average information bitrate is essentialy proportional with $P_{\rm tot}^{\rm max}$. Denoting by $N_{\rm info}^{(l)}$ the number of information bits per multicarrier symbol on the lth TP, and assuming that the power gain-to-noise ratio profile is essentially flat around its maximum, we show in appendix A that $N_{\rm info}^{(l)}$ can be approximated for small $P_{\rm tot}^{\rm max}$ as
$$N_{\rm info}^{(l)} \approx r_{\rm c}\frac{\beta_{\rm max}^{(l)}E_{\rm tot}^{\rm max}}{\gamma_{\rm thr}(1)} \qquad (8)$$
where $\beta_{\rm max}^{(l)} = \max_n \beta_n^{(l)}$. Fig. 6 shows that the dashed lines, which correspond to the approximation (8), are close to the average information bitrate at low $P_{\rm tot}^{\rm max}$, for all three coderates. For the considered LDPC codes with rates 1/2, 2/3 and 5/6, the ratio $r_{\rm c}/\gamma_{\rm thr}(1)$ equals 0.6389, 0.5232 and 0.3933, respectively, which indicates that, at small $P_{\rm tot}^{\rm max}$, the rate-1/2 code yields the larger information bitrate among these codes. Taking the information bitrate of the rate-1/2 code as a reference, the rate-2/3 and rate-5/6 codes perform worse by about 18% and 38 %, respectively.
- The rate-2/3 code provides a higher information bitrate than the other two codes only in the interval $P_{\rm tot}^{\rm max} \in (-49\,{\rm dBm}, -35\,{\rm dBm})$, where its performance is close to that of the other codes. The rate-1/2 and rate-5/6 codes outperform the rate-2/3 code for $P_{\rm tot}^{\rm max}$ < -49 dBm and $P_{\rm tot}^{\rm max}$ > -35 dBm, respectively.

When the RA is based on the SGA, the behavior of the average information bitrate versus $P_{\rm tot}^{\rm max}$ is similar to the case of threshold-based RA, the only difference being the substitution of the SNR thresholds by their LS/LB standard/modified SGA. Denoting by $R_{\rm thr}$ and $R_{\rm SGA}$ the average information bitrates resulting from threshold-based RA and SGA-based RA for a given code, Figs. 9-7 show the relative rate loss $1-\frac{R_{\rm SGA}}{R_{\rm thr}}$ as a function of $P_{\rm tot}^{\rm max}$ for the different SGAs considered, for the LDPC codes with rates 1/2, 2/3 and 5/6, respectively. A positive rate loss (i.e., $R_{\rm SGA} < R_{\rm thr}$) for a given $P_{\rm tot}^{\rm max}$ and given SGA indicates that the RA using the considered $P_{\rm tot}^{\rm max}$ and SGA yielded a lower average information bitrate compared to the RA using the exact SNR thresholds $\gamma_{\rm thr}(\mu)$. When the average information bitrate resulting from SGA-based RA is larger than the one resulting from threshold-based RA (i.e., $R_{\rm SGA} > R_{\rm thr}$), the rate loss is positive.

- In the limit for large $P_{\rm tot}^{\rm max}$, the rate loss converges to zero, because all subcarriers on all TPs are loaded with 12-bit constellations, irrespective of whether the RA is based on the SNR thresholds or on their SGA.
- In the limit for small $P_{\rm tot}^{\rm max}$, if follows from (8) that the rate loss converges to $1-\frac{\gamma_{\rm thr}(1)}{\gamma_{\rm SGA}(1)}$, where $\gamma_{\rm SGA}(1)$ represents $\gamma_{\rm stgap,LS}(1)$, $\gamma_{\rm stgap,LB}(1)$, $\gamma_{\rm modgap,LS}(1)$ or $\gamma_{\rm modgap,LB}(1)$, depending on the considered SGA. Hence, the rate loss at small $P_{\rm tot}^{\rm max}$ is positive when $\gamma_{\rm SGA}(1) > \gamma_{\rm thr}(1)$, and negative when $\gamma_{\rm SGA}(1) < \gamma_{\rm thr}(1)$. For the rate-2/3 code, it is easily verified from Fig. 8 that the sign of the rate loss at small $P_{\rm tot}^{\rm max}$ for the different SGAs is in agreement with the sign of the corresponding $\gamma_{\rm SGA}(1)-\gamma_{\rm thr}(1)$. Fig. 3 shows that the latter sign is positive for the LB standard and LB modified SGAs, negative for the LS standard SGA, and that $\gamma_{\rm modgap,LB}(1)=\gamma_{\rm thr}(1)$ (which indicates that the rate loss for the LB modified SGA goes to zero for very small $P_{\rm tot}^{\rm max}$). The signs of the rate losses at small $P_{\rm tot}^{\rm max}$, corresponding to the various SGAs for the rate-1/2 and rate-5/6 codes, are the same as for the rate 2/3 code; the only exception is the LS standard SGA, giving rise to a negative rate loss for the rate-5/6 code (this code yields $\gamma_{\rm stgap,LS}(1) < \gamma_{\rm thr}(1)$), whereas the loss is positive for the other two codes.
- For intermediate values of $P_{\rm tot}^{\rm max}$, the behavior of the rate loss versus $P_{\rm tot}^{\rm max}$ depends on the constellation sizes μ_n and the corresponding values of the considered $\gamma_{\rm SGA}(\mu_n)$ on all subcarriers. As the SGA deviates from the SNR threshold (see Fig. 3), the SGA-based RA and the threshold-based RA in general yield different bitloadings, and, therefore, different information bitrates. When, on a given subcarrier, the former RA gives rise to a constellation size which is smaller (larger) than with the latter RA, this subcarrier provides a smaller (larger) contribution to the information bitrate, compared to threshold-based RA. A positive (negative)

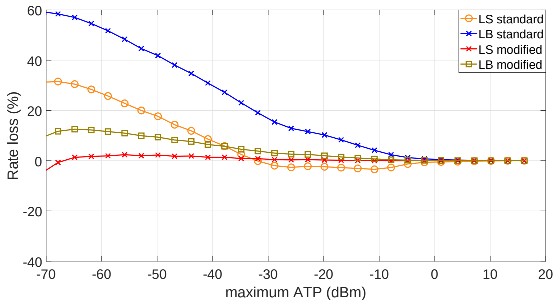

Figure 7: Relative rate loss (compared to threshold-based RA) for LDPC(1920, 960).

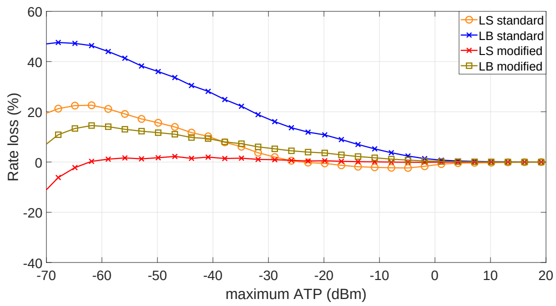

Figure 8: Relative rate loss (compared to threshold-based RA) for LDPC(1440, 960).

rate loss indicates that the dominant effect on the information bitrate comes from the constellations with a smaller (larger) size, compared to threshold-based RA.

- As $\gamma_{\mathrm{thr}}(\mu) \leq \gamma_{\mathrm{modgap,LB}}(\mu) \leq \gamma_{\mathrm{stgap,LB}}(\mu)$ by construction, both the standard LB SGA and the modified LB SGA give rise to a positive rate loss over the entire range of $P_{\mathrm{tot}}^{\max}$, with the standard LB SGA yielding the larger loss.
- As a_{LS} is decreasing with the code rate (see Table 2), the smaller code rates have SNR threshold values $\gamma_{\mathrm{thr,dB}}(\mu)$ exhibiting a larger slope when plotted versus μ_{info}. Hence, the deviations of the LS standard SGA and the LB standard SGA from the SNR thresholds get larger for smaller code rates. As a consequence, the magnitudes of the rate losses associated with the LS standard SGA and the LB standard SGA are larger for the smaller code rates.

B. BER PERFORMANCE OF SGA-BASED AND THRESHOLD-BASED RA

To avoid time-consuming simulations associated with very low BER values, the BER performance is estimated by means of a semi-analytical method, outlined in Appendix B. The accuracy of this method is assessed in Fig. 10, which compares the BERs obtained by MC simulations (markers) and by the semi-analytical method (solid lines), for the case where the rate-2/3 LDPC code is used, and the RA is based

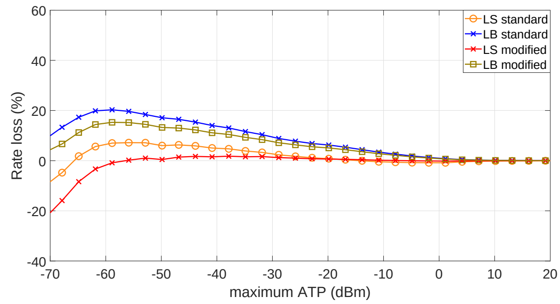

Figure 9: Relative rate loss (compared to threshold-based RA) for LDPC(1152, 960).

on the SNR thresholds and on the various SGAs; to limit the simulation time, we only considered a range of $P_{\mathrm{tot}}^{\max}$ where the BER is near 10^{-5} or larger.

For the considered LDPC codes with rates 1/2, 2/3 and 5/6, Figs. 11-13 display the (semi-analytical) BER versus the maximum ATP, $P_{\mathrm{tot}}^{\max}$, resulting from RA based on the SNR thresholds and on the various SGAs.

- For threshold-based RA, the BER essentially equals the reference value of 10^{-5} over the entire range of $P_{\mathrm{tot}}^{\max}$.
- For very large $P_{\mathrm{tot}}^{\max}$, the energy $E_n^{(l)}$ on the nth subcarrier from the lth TP is selected such that $\beta_n^{(l)} E_n^{(l)} = \gamma(\mu_{\max})$, where $\beta_n^{(l)}$ is the corresponding power gain-to-noise ratio, and $\gamma(\mu)$ stands for $\gamma_{\mathrm{thr}}(\mu)$ (in the case of threshold-based RA) or $\gamma_{\mathrm{SGA}}(\mu)$ (in the case of SGA-based RA). The BER for both the LB standard SGA and the LB modified SGA equals 10^{-5}, because the corresponding $\gamma_{\mathrm{SGA}}(\mu_{\max})$ equals $\gamma_{\mathrm{thr}}(\mu_{\max})$ (see Fig. 3 for the rate-2/3 LDPC code). The BER for both the LS standard SGA and the LS modified SGA is larger than 10^{-5}, because the corresponding $\gamma_{\mathrm{SGA}}(\mu_{\max})$ is less than $\gamma_{\mathrm{thr}}(\mu_{\max})$ (see Fig. 3 for the rate-2/3 LDPC code): $E_n^{(l)}$ is too small to achieve BER = 10^{-5} for $\mu = \mu_{\max}$. The LS standard SGA yields the larger BER (larger than 10^{-5} by several orders of magnitude), because $\gamma_{\mathrm{stgap,LS}}(\mu_{\max}) < \gamma_{\mathrm{modgap,LS}}(\mu_{\max})$.
- For very small $P_{\mathrm{tot}}^{\max}$, we have BER > 10^{-5} when $\gamma_{\mathrm{SGA}}(1) < \gamma_{\mathrm{thr}}(1)$. This is the case for (i) the LS modified SGA for all three codes, and (ii) the LS standard SGA for the rate-5/6 code), all giving rise to a BER which exceeds 10^{-5} by several orders of magnitude. We obtain BER < 10^{-5} when $\gamma_{\mathrm{SGA}}(1) > \gamma_{\mathrm{thr}}(1)$, which is is the case for (i) the LB standard SGA for all three codes, and (ii) the LS standard SGA for the rate-1/2 and rate-2/3 codes. For all three codes, $\gamma_{\mathrm{modgap,LB}}(1) = \gamma_{\mathrm{thr}}(1)$, so that the BER associated with the LB modified SGA converges to 10^{-5} in the limit for very small $P_{\mathrm{tot}}^{\max}$.
- For intermediate values of $P_{\mathrm{tot}}^{\max}$, the behavior of the BER versus $P_{\mathrm{tot}}^{\max}$ depends on the constellation sizes μ_n and the corresponding values of the considered

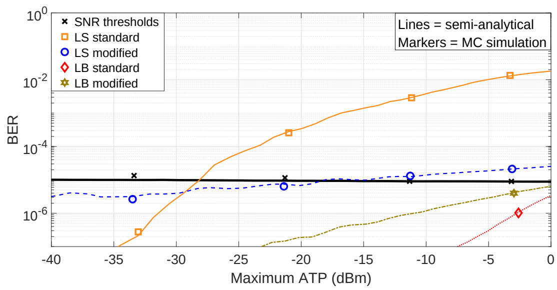

Figure 10: BER on the 1st TP for LDPC(1440, 960). MC simulations (markers) agree with the semi-analytical BER (lines).

$\gamma_{\mathrm{SGA}}(\mu_n)$ on all subcarriers. For the LS standard and LS modified SGAs, a BER larger (smaller) than 10^{-5} for a given $P_{\mathrm{tot}}^{\max}$ and given SGA indicates that, for the considered $P_{\mathrm{tot}}^{\max}$, the majority of the constellations in the multicarrier symbol have a SNR threshold which is larger (smaller) that the considered SGA.

- As $\gamma_{\mathrm{thr}}(\mu) \leq \gamma_{\mathrm{modgap,LB}}(\mu) \leq \gamma_{\mathrm{stgap,LB}}(\mu)$ by construction, both the LB standard SGA and the LB modified SGA give rise to smaller constellations compared to threshold-based RA, which results in BER $\leq 10^{-5}$; the LB standard SGA yields the smaller BER.

C. CONCLUDING REMARKS

If can be verified from Figs. 7-9 and Figs. 11-13 that there are no intervals of $P_{\mathrm{tot}}^{\max}$ where simultaneously the rate loss for a given SGA is negative (i.e., $R_{\mathrm{SGA}} > R_{\mathrm{thr}}$) and the corresponding BER is below 10^{-5}; this illustrates that no performance gain can be obtained by using SGA-based RA instead of threshold-based RA.

However, SGA-based RA might be preferred over threshold-based RA, because of the higher mathematical flexibility of the former. A major disadvantage of the LS standard SGA and the LS modified SGA is the considerable violation of the BER constraint, as shown in Figs. 11-13. No BER violation occurs for the LB standard SGA and the LB modified SGA, but the drawback is a rate loss compared to threshold-based RA, especially at low $P_{\mathrm{tot}}^{\max}$ (see Figs. 9-7); the LB modified SGA is to be preferred, because of its smaller rate loss. For the considered codes, the rate loss resulting from the LB modified SGA is limited to about 15%, while rate losses up to about 60% are observed for the LB standard SGA.

VI. CONCLUSIONS

RA in multicarrier systems is commonly based on SNR thresholds. While the SNR thresholds for TCM (and for uncoded transmission) are well approximated by the standard SGA, we have demonstrated that this is no longer the case for LDPC-coded modulation. Therefore, we have proposed a modified SGA for LDPC-coded modulation, which provides a substantially better fit to the SNR thresholds.

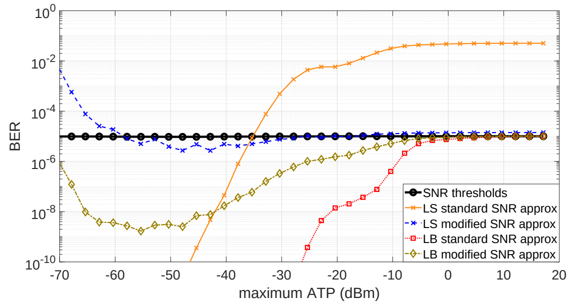

Figure 11: Average (semi-analytical) BER for LDPC(1920, 960)

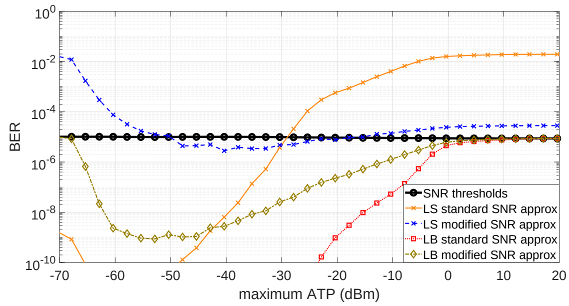

Figure 12: Average (semi-analytical) BER for LDPC(1440, 960)

Selecting the parameters of the standard and modified SGA to provide a LS fit to the SNR thresholds for LDPC-coded modulation can give rise to a considerable violation (by a few orderes of magnitude) of the BER constraint. To avoid the increased BER, we have introduced the LB standard and LB modified SGA, which are lower-bounded by the SNR thresholds. However, the drawback of these LB SGAs is a reduction of the information bitrate, compared to the RA based on the SNR thresholds. Numerical results, pertaining to a single-user scenario involving the transmission of a G.fast multicarrier signal over a TP, indicates that the rate loss resulting from the LB SGAs is very small at high TX power levels (with essentially all subcarriers carrying the largest allowed constellation). In contrast, at low TX power

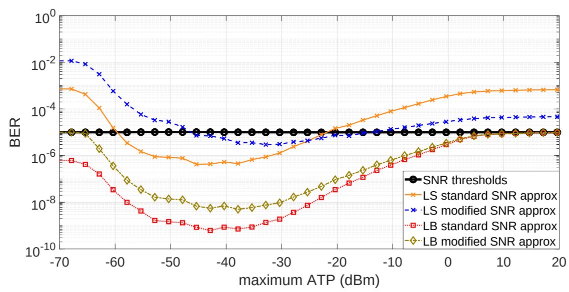

Figure 13: Average (semi-analytical) BER for LDPC(1152, 960)

levels (with mainly small constellations being used) the LB SGAs exhibit rate losses of several tens of percent; the LB modified SGA yields the smaller loss, which is limited to about 15%.

.

APPENDIX A INFORMATION BITRATES FOR SMALL ATP

Let $\boldsymbol{\beta}' = (\beta'_1, ..., \beta'_N)$ be the permutation of $\boldsymbol{\beta} = (\beta_1, ..., \beta_N)$, such that the elements of $\boldsymbol{\beta}'$ are in descending order, i.e., $\beta'_1 \geq \beta'_2 \geq ... \geq \beta'_N$. We denote by $\gamma(\mu)$ either the actual SNR threshold $\gamma_{\text{thr}}(\mu)$ or its SGA $\gamma_{\text{SGA}}(\mu)$; the latter represents $\gamma_{\text{stgap,LS}}(\mu)$, $\gamma_{\text{stgap,LB}}(\mu)$, $\gamma_{\text{modgap,LS}}(\mu)$ or $\gamma_{\text{modgap,LB}}(\mu)$. Considering that N_{info} versus $E_{\text{tot}}^{\max}$ is an increasing staircase function (which we represent as $N_{\text{info}} = g_{\text{step}}(E_{\text{tot}}^{\max})$) with vertical steps of size r_{c}, we denote by $E_{\text{tot}}^{\max}(i)$ the minimal value of $E_{\text{tot}}^{\max}$ yielding $N_{\text{info}} = ir_{\text{c}}$. We introduce the piece-wise linear function $g_{\text{lin}}(E_{\text{tot}}^{\max})$, obtained by connecting the successive points $((E_{\text{tot}}^{\max}(1), r_{\text{c}}), (E_{\text{tot}}^{\max}(2), 2r_{\text{c}}), ...)$. When the number N of subcarriers is large, the vertical steps of $g_{\text{step}}(E_{\text{tot}}^{\max})$ are very small, considering the scale in Figs. 5 and 6 (a stepsize r_{c} in N_{info} corresponds to a stepsize $r_{\text{c}}R_{\text{sy}} < R_{\text{sy}}$ = $48 \cdot 10^3$ bps in information bitrate in Figs. 5 and 6), so that $g_{\text{step}}(E_{\text{tot}}^{\max}) \approx g_{\text{lin}}(E_{\text{tot}}^{\max})$.

Achieving $N_{\text{info}} = r_{\text{c}}$ with minimal energy corresponds to placing one coded bit on the subcarrier associated with β'_1; this yields $E_{\text{tot}}^{\max}(1) = \frac{1}{\beta'_1}\gamma(1)$.

For SGA-based RA, it can be verified from (4) that $\gamma_{\text{SGA}}(2) > 2\gamma_{\text{SGA}}(1)$. With N_1 denoting the largest integer satisfying $\frac{\gamma_{\text{SGA}}(2)-\gamma_{\text{SGA}}(1)}{\beta'_1} > \frac{\gamma_{\text{SGA}}(1)}{\beta'_{N_1}}$, we have $N_1 \geq 1$. When $N_1 > 1$, it takes less energy to place a single bit on the subcarrier corresponding to β'_n (with $n = 2, ..., N_1$), than to place a second bit on the subcarrier corresponding to β'_1. Hence, we obtain

$$E_{\text{tot}}^{\max}(i) = \gamma_{\text{SGA}}(1) \sum_{n=1}^{i} \frac{1}{\beta'_n} \tag{9}$$

for $i = 1, ..., N_1$, which is achieved by placing a single bit on the subcarriers corresponding to $\beta'_1, ..., \beta'_i$.

For RA based on the SNR thresholds, one has $\gamma_{\text{thr}}(2) = 2\gamma_{\text{thr}}(1)$ (because the 1-bit and 2-bit constellations are (a rotated version of) BPSK and 4-QAM, respectively) and $\gamma_{\text{thr}}(3) > 3\gamma_{\text{thr}}(1)$. With N_2 denoting the largest integer satisfying $\frac{\gamma_{\text{thr}}(3)-2\gamma_{\text{thr}}(1)}{\beta'_1} > \frac{\gamma_{\text{thr}}(1)}{\beta'_{N_2}}$, we have $N_2 \geq 1$. When $N_2 > 1$, it takes less energy to place a first bit or add a second bit on the subcarrier corresponding to β'_n (with $n = 2, ..., N_2$), than to place a third bit on the subcarrier corresponding to β'_1. This yields

$$E_{\text{tot}}^{\max}(2i) = 2\gamma_{\text{thr}}(1) \sum_{n=1}^{i} \frac{1}{\beta'_n} \tag{10}$$

for $i = 1, ..., N_2$, and

$$E_{\text{tot}}^{\max}(2i+1) = 2\gamma_{\text{thr}}(1) \sum_{n=1}^{i} \frac{1}{\beta'_n} + \gamma_{\text{thr}}(1)\frac{1}{\beta'_{i+1}} \tag{11}$$

for $i = 1, ..., N_2 - 1$. We achieve (10) by placing two bits on the subcarriers corresponding to $\beta'_1, ..., \beta'_i$; (11) is achieved by additionally placing one bit on the subcarrier corresponding to β'_{i+1}.

When the power gain-to-noise ratio profile is essentially flat around its maximum value, inside an interval of N_{fl} subcarrier spacings, we have $\beta'_n \approx \beta'_1$ for $n = 2, ..., N_{\text{fl}}+1$; as a consequence, $N_1 \geq N_{\text{fl}} + 1$ and $N_2 \geq N_{\text{fl}} + 1$. In this case, (9) and (10)-(11) reduce to $E_{\text{tot}}^{\max}(i) \approx i\frac{\gamma(1)}{\beta'_1}$, for $i = 1, ..., N_{\text{fl}}+1$ and for $i = 1, ..., 2(N_{\text{fl}}+1)$, respectively. This yields $g_{\text{lin}}(E_{\text{tot}}^{\max}) \approx \frac{r_{\text{c}}\beta'_1}{\gamma(1)}E_{\text{tot}}^{\max}$ for $E_{\text{tot}}^{\max} \leq \frac{\gamma(1)}{\beta'_1}(N_{\text{fl}}+1)$ (SGA-based RA) or $E_{\text{tot}}^{\max} \leq 2\frac{\gamma(1)}{\beta'_1}(N_{\text{fl}}+1)$ (threshold-based RA).

APPENDIX B SEMI-ANALYTICAL BER ESTIMATION FOR LDPC CODING

For the case of a uniform bitloading and SNR profile ($\boldsymbol{\mu} = \mu\mathbf{1}_N$ and $\boldsymbol{\gamma} = \gamma\mathbf{1}_N$), the following tables are constructed for $\mu \in \{1, 2, ..., \mu_{\max}\}$: (i) the BER versus γ, resulting from MC simulation of the LDPC decoder for given μ, i.e., $\log_{10}(\text{BER}) = f_\mu(\gamma)$; (ii) the average MI (between a coded bit and its log-likelihood ratio [26]) per bit versus γ for given μ, i.e., $I_{\text{bit}} = g_\mu(\gamma)$; and (iii) the BER versus the MI per bit for given μ, i.e., $\log_{10}(\text{BER}) = h_\mu(I_{\text{bit}})$, which is obtained from the tables (i) and (ii) as $\log_{10}(\text{BER}) = f_\mu(g_\mu^{-1}(I_{\text{bit}}))$, with $g_\mu^{-1}(.)$ denoting the inverse function of $g_\mu(.)$. As shown empirically in [27], the function $h_\mu(.)$ depends only weakly on μ.

The BER estimate resulting from a bitloading $\boldsymbol{\mu} = (\mu_1, ..., \mu_N)$ and SNR profile $\boldsymbol{\gamma} = (\gamma_1, ..., \gamma_N)$ is obtained in two steps. First, the average MI per bit for the considered $\boldsymbol{\mu}$ and $\boldsymbol{\gamma}$ is computed as

$$I_{\text{bit,avg}} = \frac{\sum_{n=1}^{N} \mu_n g_{\mu_n}(\gamma_n)}{\sum_{n=1}^{N} \mu_n} \tag{12}$$

Next, the BER estimate BER_{est} is obtained from

$$\log_{10}(\text{BER}_{\text{est}}) = \frac{\sum_{n=1}^{N} \mu_n h_{\mu_n}(I_{\text{bit,avg}})}{\sum_{n=1}^{N} \mu_n} \tag{13}$$

Note that (13) provides the exact BER value when the bitloading and the SNR profile are uniform: indeed, in this case, (12) and (13) reduce to $I_{\text{bit,avg}} = g_\mu(\gamma)$ and $\log_{10}(\text{BER}_{\text{est}}) = h_\mu(g_\mu(\gamma)) = f_\mu(\gamma)$, respectively, so that $\log_{10}(\text{BER}_{\text{est}}) = \log_{10}(\text{BER})$.

References

[1] R. V. Sonalkar and R. R. Shively, "An efficient bit-loading algorithm for DMT applications," IEEE Communications Letters, vol. 4, no. 3, pp. 80–82, 2000.

[2] D. Hughes-Hartogs, "Ensemble modem structure for imperfect transmission media," Oct. 1 1991. US Patent 5,054,034.
[3] E. Baccarelli and M. Biagi, "Optimal integer bit-loading for multicarrier ADSL systems subject to spectral-compatibility limits," Signal processing, vol. 84, no. 4, pp. 729–741, 2004.
[4] A. Fasano, "On the optimal discrete bit loading for multicarrier systems with constraints," in Vehicular Technology Conference, 2003. VTC 2003-Spring. The 57th IEEE Semiannual, vol. 2, pp. 915–919, IEEE, 2003.
[5] B. Krongold, K. Ramchandran, and D. Jones, "Computationally efficient optimal power allocation algorithms for multicarrier communication systems," IEEE Transactions on Communications, vol. 48, pp. 23–27, 2000.
[6] R. Cendrillon, W. Yu, M. Moonen, J. Verlinden, and T. Bostoen, "Optimal multiuser spectrum balancing for digital subscriber lines," IEEE Transactions on Communications, vol. 54, no. 5, pp. 922–933, 2006.
[7] P. Tsiaflakis, J. Vangorp, J. Verlinden, and M. Moonen, "Multiple access channel optimal spectrum balancing for upstream DSL transmission," IEEE Communications Letters, vol. 11, no. 4, pp. 398–400, 2007.
[8] A. R. Forouzan, M. Moonen, J. Maes, and M. Guenach, "Joint level 2 and 3 dynamic spectrum management for upstream VDSL," IEEE Transactions on Communications, vol. 59, no. 10, pp. 2851–2861, 2011.
[9] C. M. Akujuobi, J. Shen, and M. N. Sadiku, "A new parallel greedy bit-loading algorithm with fairness for multiple users in a DMT system," IEEE Transactions on Communications, vol. 54, no. 8, pp. 1374–1380, 2006.
[10] D. Zanatta Filho, R. R. Lopes, R. Ferrari, R. Suyama, and B. Dortschy, "Bit loading for precoded DSL systems," in Acoustics, Speech and Signal Processing, 2007. ICASSP 2007. IEEE International Conference on, vol. 3, pp. 353–356, IEEE, 2007.
[11] G. D. Forney and M. V. Eyuboglu, "Combined equalization and coding using precoding," IEEE Communications Magazine, vol. 29, no. 12, pp. 25–34, 1991.
[12] P. S. Chow, J. M. Cioffi, and J. A. Bingham, "A practical discrete multitone transceiver loading algorithm for data transmission over spectrally shaped channels," IEEE Transactions on Communications, vol. 43, no. 234, pp. 773–775, 1995.
[13] M. Chiang, C. W. Tan, D. P. Palomar, D. O'Neill, and D. Julian, "Power control by geometric programming," IEEE Transactions on Wireless Communications, vol. 6, no. 7, pp. 2640–2651, 2007.
[14] P. Tsiaflakis, M. Diehl, and M. Moonen, "Distributed spectrum management algorithms for multiuser DSL networks," IEEE Transactions on Signal Processing, vol. 56, no. 10, pp. 4825–4843, 2008.
[15] J. Papandriopoulos and J. S. Evans, "SCALE: A low-complexity distributed protocol for spectrum balancing in multiuser DSL networks," IEEE Transactions on Information Theory, vol. 55, no. 8, pp. 3711–3724, 2009.
[16] R. B. Moraes, M. Wolkerstorfer, P. Tsiaflakis, and M. Moonen, "Dynamic spectrum management with spherical coordinates.," IEEE Transactions on Signal Processing, vol. 62, no. 21, pp. 5589–5602, 2014.
[17] W. Lanneer, P. Tsiaflakis, J. Maes, and M. Moonen, "Linear and nonlinear precoding based dynamic spectrum management for downstream vectored G.fast transmission," IEEE Transactions on Communications, vol. 65, no. 3, pp. 1247–1259, 2017.
[18] J. Verdyck and M. Moonen, "Dynamic spectrum management in digital subscriber line networks with unequal error protection requirements," IEEE Access, vol. 5, pp. 18107–18120, 2017.
[19] V. M. Chan and W. Yu, "Multiuser spectrum optimization for discrete multitone systems with asynchronous crosstalk," IEEE Transactions on Signal Processing, vol. 55, no. 11, pp. 5425–5435, 2007.
[20] F. Gianaroli, F. Pancaldi, and G. M. Vitetta, "A novel bit and power loading algorithm for narrowband indoor powerline communications," in Communication Workshop (ICCW), 2015 IEEE International Conference on, pp. 1557–1562, IEEE, 2015.
[21] T. N. Vo, K. Amis, T. Chonavel, and P. Siohan, "Achievable throughput optimization in OFDM systems in the presence of interference and its application to power line networks," IEEE Transactions on Communications, vol. 62, no. 5, pp. 1704–1715, 2014.
[22] T. N. Vo, K. Amis, T. Chonavel, and P. Siohan, "A computationally efficient discrete bit-loading algorithm for OFDM systems subject to spectral-compatibility limits," IEEE Transactions on Communications, vol. 63, no. 6, pp. 2261–2272, 2015.
[23] "ITU-T recommendation G.9701: Fast access to subscriber terminals (G.fast) - physical layer specification," March 2019.
[24] P. Golden, H. Dedieu, and K. S. Jacobsen, Fundamentals of DSL technology. CRC Press, 2005.
[25] "ITU-T recommendation G.9960: Unified high-speed wireline-based home networking transceivers - system architecture and physical layer specification," April 2018.
[26] W. Ryan and S. Lin, Channel codes: classical and modern. Cambridge University Press, 2009.
[27] Y. Li and W. E. Ryan, "Mutual-information-based adaptive bit-loading algorithms for LDPC-coded OFDM," IEEE Transactions on Wireless Communications, vol. 6, no. 5, pp. 1670–1680, 2007.
[28] G. Scutari, F. Facchinei, P. Song, D. P. Palomar, and J.-S. Pang, "Decomposition by partial linearization: Parallel optimization of multi-agent systems," IEEE Transactions on Signal Processing, vol. 62, no. 3, pp. 641–656, 2014.

[29] TNO, "G.fast: Release of measured transfer characteristics of the 104m KPN access cable." https://www.joepeesoft.com/Public/DSL_Corner/_Index.html, 2013.

ADRIAAN SULS (S'15) received the M.Sc. degree in electrical engineering from Ghent University, Ghent, Belgium, in 2013. Afterwards, he started pursuing his Ph.D. degree with the Department of Telecommunications and Information Processing (TELIN) of Ghent University under the supervision of Prof. M. Moeneclaey.

His research interests include channel coding and DSL wireline access networks with a special interest in LDPC codes.

JEROEN VERDYCK (S'15) received the M.Sc. degree in electrical engineering from KU Leuven, Leuven, Belgium, in 2014, where he is currently pursuing the Ph.D. degree with the Electrical Engineering Department, under the supervision of Prof. M. Moonen. He is involved in joint projects with KU Leuven and University of Antwerp, Antwerp, Belgium.

His research interests include signal processing and optimization for digital communication systems with an emphasis on DSL wireline access networks.

MARC MOONEN (M'94–S'06–F'07) is a Full Professor at the Electrical Engineering Department of KU Leuven, where he is heading a research team working in the area of numerical algorithms and signal processing for digital communications, wireless communications, DSL and audio signal processing.

He is a Fellow of the IEEE (2007) and a Fellow of EURASIP (2018).

He received the 1994 KU Leuven Research Council Award, the 1997 Alcatel Bell (Belgium) Award (with Piet Vandaele), the 2004 Alcatel Bell (Belgium) Award (with Raphael Cendrillon), and was a 1997 Laureate of the Belgium Royal Academy of Science. He received journal best paper awards from the IEEE Transactions on Signal Processing (with Geert Leus and with Daniele Giacobello) and from Elsevier Signal Processing (with Simon Doclo).

He was chairman of the IEEE Benelux Signal Processing Chapter (1998-2002), a member of the IEEE Signal Processing Society Technical Committee on Signal Processing for Communications, and President of EURASIP (European Association for Signal Processing, 2007-2008 and 2011-2012).

He has served as Editor-in-Chief for the EURASIP Journal on Applied Signal Processing (2003-2005), Area Editor for Feature Articles in IEEE Signal Processing Magazine (2012-2014), and has been a member of the editorial board of Signal Processing, IEEE Transactions on Circuits and Systems II, IEEE Signal Processing Magazine, Integration-the VLSI Journal, EURASIP Journal on Wireless Communications and Networking and EURASIP Journal on Advances in Signal Processing.

MARC MOENECALEY (M'93–SM'99–F'02) is Full Professor at the Telecommunications and Information Processing (TELIN) Department, Ghent University, teaching courses on various aspects of Digital Communications.

His main research interests are in statistical communication theory, carrier and symbol synchronization, bandwidth-efficient modulation and coding, spread-spectrum, satellite and mobile communication. He is the author of more than 500 scientific papers in international journals and conference proceedings. Together with Prof. H. Meyr and Dr. S. Fechtel , he co-authors the book Digital communication receivers – Synchronization, channel estimation, and signal processing.(J. Wiley, 1998). He is co-recipient of the Mannesmann Innovations Prize 2000. He is a Highly Cited Researcher 2001. In 2002 he was elected to the grade of Fellow of the IEEE.

During the period 1992-1994, he was Editor for Synchronization, for the IEEE Transactions on Communications. He served as co-guest editor for special issues of the Wireless Personal Communications Journal (on Equalization and Synchronization in Wireless Communications) and the IEEE Journal on Selected Areas in Communications (on Signal Synchronization in Digital Transmission Systems) in 1998 and 2001, respectively.